Dalton Transactions

Cite this: *Dalton Trans.*, 2011, **40**, 431

www.rsc.org/dalton

PAPER

'Double redox-activity' in azobenzene-quinonoid palladium(II) complexes: a combined structural, electrochemical and spectroscopic study†

Naina Deibel,[a] David Schweinfurth,[a] Ralph Huebner,[a] Pierre Braunstein*[b] and Biprajit Sarkar*[a]

Received 2nd August 2010, Accepted 12th October 2010
DOI: 10.1039/c0dt00944j

Reactions of $[(\mathbf{az}_{-H})Pd(\mu\text{-}Cl)_2Pd(\mathbf{az}_{-H})]$ (**az** = azobenzene) with the zwitterionic, *p*-benzoquinonemonoimine-type ligands 4-(*n*-butylamino)-6(*n*-butylimino)-3-oxocyclohexa-1,4-dien-1-olate (**Q**[1]) or 4-(isopropylamino)-6(isopropylimino)-3-oxocyclohexa-1,4-dien-1-olate) (**Q**[2]) in the presence of a base leads to the formation of the mononuclear complexes $[(\mathbf{az}_{-H})Pd(\mathbf{Q}^1{}_{-H})]$ (**1**) and $[(\mathbf{az}_{-H})Pd(\mathbf{Q}^2{}_{-H})]$ (**2**) respectively. Structural characterization of **2** shows an almost square planar coordination geometry around the Pd(II) centre, a short Pd–C bond, a slight elongation of the N=N double bond of the $\mathbf{az}_{-H}$ ligand and localization of the double bonds within the $\mathbf{Q}^2{}_{-H}$ ligand. Additionally, intermolecular N–H–O interactions exist between the uncoordinated N–H and O groups of two different molecules. Cyclic voltammetry of the complexes reveals an irreversible oxidation and two reversible reduction processes. A combination of electrochemical and UV-vis-NIR and EPR spectroelectrochemical studies are used to show that both coordinated ligands participate successively in the redox processes, thus revealing their non-innocent character.

Introduction

Azobenzene (**az**) is an interesting molecule owing to its ability to show photo- or redox-induced isomerism in its free as well as metal coordinated forms.[1–3] One of the first studies on C–H activation by metal complexes was done with Pd(II) and Pt(II) complexes of azobenzene and resulted in *C*, *N*-cyclometallation.[4,5] Azo-ligands have been well established as non-innocent ligands in coordination chemistry.[6,7] Most of the metal complexes studied in that regard contain either phenylazopyridine (pap)[8–11] or 2,2′-azobispyridine (abpy)[12,13] as ligands because of the increased stability brought about by the presence of one or more pyridine rings. The use of azobenzene as a non-innocent ligand has been rarely seen or explored. Quinonoid compounds, in contrast represent a class of ligands which have been recognized for their non-innocent character.[14,15] Not only are ligands such as dioxolene[16,17] and dithiolene[18–20] non-innocent but also the potentially bridging ligand 1,4-dihydroxy benzoquinone[21,22] and various substituted derivatives thereof.[23–25] In this context, we have investigated ligands of form **Q** (Scheme 1) which are zwitterionic, benzoquinonemonoimine-type compounds containing two delocalized but mutually isolated 6π systems.[26–29]

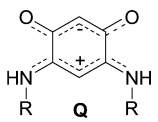

Scheme 1 A zwitterionic quinonoid ligand.

These ligands have shown interesting properties in supramolecular chemistry,[29] homogenous catalysis,[30,31] mediators for "metal–metal coupling"[32,33] and most recently as non-innocent ligands in combination with copper.[34,35] Cu(I) complexes with potentially bridging quinonoid ligands are rare[36] and we recently reported on mono-[34] and dinuclear complexes of such ligands.[35] The *para*-isomers of these ligands have also been popularized in recent years.[37–40] Herein we present two metal complexes, $[(\mathbf{az}_{-H})\mathbf{Pd}(\mathbf{Q}^1{}_{-H})]$ (**1**) and $[(\mathbf{az}_{-H})\mathbf{Pd}(\mathbf{Q}^2{}_{-H})]$ (**2**), which combine the cyclometallated form of azobenzene together with the mono deprotonated form of the ligands, 4-(*n*-butylamino)-6(*n*-butylimino)-3-oxocyclohexa-1,4-dien-1-olate (**Q**[1]) and 4-(isopropylamino)-6(isopropylimino)-3-oxocyclohexa-1,4-dien-1-olate) (**Q**[2]) respectively. Results obtained from ^{1}H-NMR spectroscopy, elemental analyses and X-ray crystallography are used for the formulation of the products. A combination of electrochemical and UV-vis-NIR and EPR spectroelectrochemical methods are applied to establish the non-innocent nature of both these ligands in the aforementioned complexes.

[a]*Institut für Anorganische Chemie, Universität Stuttgart, Pfaffenwaldring 55, D-70550, Stuttgart, Germany. E-mail: sarkar@iac.uni-stuttgart.de*
[b]*Laboratoire de Chimie de Coordination, Institut de Chimie (UMR 7177 CNRS), Université de Strasbourg, 4 rue Blaise Pascal, F-67081, Strasbourg Cedex, France. E-mail: braunstein@unistra.fr; Fax: (+)33368851322; Tel: (+)33368851308*

† Electronic supplementary information (ESI) available: Cyclic voltammogram of **1**, changes in the UV-vis-NIR spectra of **2** during reduction processes, EPR spectrum of $\mathbf{2}^{\bullet-}$. CCDC reference numbers 784390. For ESI and crystallographic data in CIF or other electronic format see DOI: 10.1039/c0dt00944j

Results and discussion

Syntheses and crystal structure of 2

The compounds **1** and **2** were synthesized by reacting [(**az**$_{-H}$)Pd(μ-Cl)$_2$Pd(**az**$_{-H}$)] with the ligands **Q**^{1} or **Q**^{2}, respectively, which were deprotonated by the addition of a base prior to the addition of the metal precursor (Scheme 2). The reactions proceeded smoothly at room temperature and analytically pure deep brown solids were isolated in reasonable yields after recrystallisation. The purity of the complexes was established by using ^{1}H-NMR spectroscopy and elemental analyses.

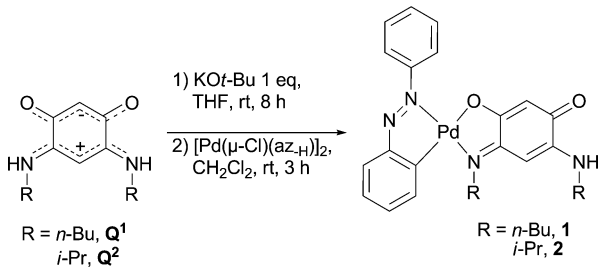

Scheme 2 Synthesis of the complexes.

Compound **2** was crystallized by slow evaporation of a dichloromethane solution of the complex layered with *n*-hexane (1/4) at ambient temperature. It crystallises in the monoclinic *C*2/*c* space group. An ORTEP diagram of **2** is shown in Fig. 1, crystallographic details are presented in Table 1 and selected bond lengths and angles in are given in Table 2.

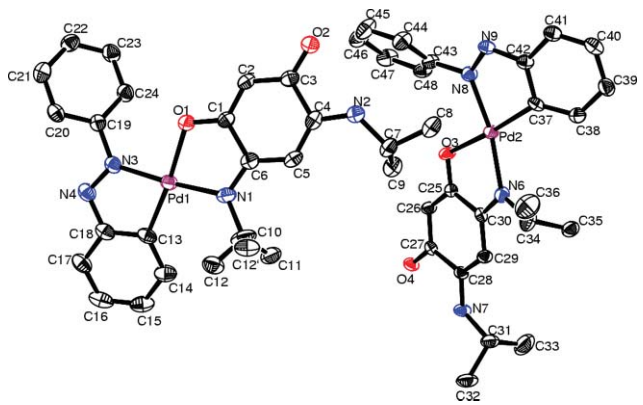

Fig. 1 ORTEP view of **2**. Ellipsoids are drawn at 30% probability. Asymmetric unit contains two molecules. Hydrogen atoms are omitted for clarity.

The Pd centre is in a slightly distorted square planar environment, being coordinated by the C$^-$ and azo N atoms of the cyclometallated **az**$_{-H}$ ligand and by oxygen and nitrogen atoms of the **Q**$^2_{-H}$ ligand. The distortion is imposed by the chelating nature of the two ligands and accordingly the O1–Pd1–N1 and C13–Pd1–N3 angles are smaller (78.8(1) and 78.5(1)°, respectively) than the N3–Pd1–O1 and C13–Pd1–N1 angles (95.2(1) and 107.7(1)°, respectively). The Pd1–C13 distance at 1.995(3) Å is relatively short as would be expected for a σ-bond between a C$^-$ atom of a phenyl ring and a Pd(II) centre. Accordingly the Pd1–O1 (2.058(2) Å) distance which is *trans* to Pd1–C13 is relatively long

Table 1 Crystallographic Details

Chemical formula	$C_{48}H_{52}N_8O_4Pd_2$
M_r	1017.78
Crystal system, space group	Monoclinic, *C*2/*c*
T/K	150
a, *b*, *c*/Å	23.6552(13), 25.0045(11), 17.5305(11)
β (°)	120.109(8)
V/Å^3	8970.0(8)
Z	8
Density/g cm^{-3}	1.507
F000	4160
Radiation type	Mo-Kα
μ/mm^{-1}	0.855
Crystal size/mm	0.32 × 0.27 × 0.23
meas. refl.	35155
indep. refl.	7895
obsvd. [$I > 2\sigma(I)$] refl.	6396
R_{int}	0.116
$R[F^2 > 2\sigma(F^2)]$, $wR(F^2)$, *S*	0.040, 0.092, 1.035
$\Delta\rho_{max}$, $\Delta\rho_{min}$/e Å^{-3}	1.63, –0.661

Table 2 Selected bond lengths (Å) and bond angles (°) of one of the two molecules in the asymmetric unit of **2** and of **Q**^{2}

Bond Lengths	**2**	**Q**^{2}
Pd1–O1	2.058(2)	
Pd1–C13	1.995(3)	
Pd1–N3	2.018(3)	
Pd1–N1	2.078(3)	
C1–O1	1.286(4)	1.251(2)
C3–O2	1.236(4)	1.252(2)
C1–C2	1.363(5)	1.398(2)
C2–C3	1.404(5)	1.401(2)
C3–C4	1.519(5)	1.533(2)
C4–C5	1.371(5)	1.393(2)
C5–C6	1.411(5)	1.395(2)
C6–C1	1.509(5)	1.538(2)
C6–N1	1.317(5)	1.321(2)
C4–N2	1.331(5)	1.322(2)
N3–N4	1.269(4)	
N3–C19	1.437(4)	
N4–C18	1.398(5)	
Bond Angles		
O1–Pd1–N1	78.8(1)	
N1–Pd1–C13	107.7(1)	
C13–Pd1–N3	78.5(1)	
N3–Pd1–O1	95.2(1)	
N3–Pd1–N1	172.1(1)	
C13–Pd1–O1	173.5(1)	

(*trans* influence). The Pd1–N3 distance of 2.018(3) Å is shorter than the Pd1–N1 distance of 2.078(3) Å. The π-acceptor character of the azo ligand results in back donation from the Pd(II) centre and accounts for the shortening of the Pd1–N3 bond.[13] Such an effect is absent in the imino type N1 donor and hence the Pd1–N1 distance is longer. The N3–N4 distance of 1.269(4) Å is slightly longer than a typical N=N double bond distance of 1.25 Å in an azo compound. This elongation is related to back donation from the Pd(II) centre into the π* orbital of the **az**$_{-H}$ ligand.[6,13] In keeping with this the N4–C18 distance of 1.398(5) Å is shorter than the N3–C19 distance of 1.437(4) Å. Averaging out of bond distances within the chelate ring is a typical feature of metal complexes containing azo ligands.[13] The uncoordinated phenyl ring is twisted with respect to the rest of the molecule. The dihedral angle between the plane of the uncoordinated phenyl ring and the mean coordination plane of the Pd centre is 41.2°. The phenyl ring is possibly twisted

due to packing effects. Analysis of the bond lengths within the $\mathbf{Q^2}_{\text{-H}}$ ligand reveals that the C1–O1 distance at 1.286(4) Å is longer than the C3–O2 distance of 1.236(4) Å. Accordingly, the C1–C2 distance of 1.363(5) Å is shorter than the C2–C3 distance of 1.404(5). For comparison the free ligand $\mathbf{Q^2}$ has distances of 1.251(2) and 1.252(2) Å for C1–O1 and C3–O2 respectively and 1.398(2) and 1.401(2) Å, for C1–C2 and C2–C3 respectively.[34] The C6–N1 and C4–N2 distances in **2** are 1.317(5) and 1.331(5) Å, respectively and the C5–C6 and C4–C5 distances are 1.411(5) and 1.371(5) Å, respectively. For comparison, relevant bond distances within the free ligand $\mathbf{Q^2}$ are C6–N1, 1.321(2); C4–N2, 1.322(2); C5–C6, 1.395(2); and C4–C5, 1.393(2) Å. These results show that whereas the double bonds in the "upper" and "lower" parts of the molecule are delocalized in the free ligand $\mathbf{Q^2}$,[34] these bonds become more localized on coordination to one metal centre. Such metal-induced localization of the double bonds has been observed previously for related systems.[30,34] The C1–C6 and C3–C4 distances of 1.509(5) and 1.519(5) Å, respectively for **2** and 1.538(2) and 1.533(2) Å, respectively for $\mathbf{Q^2}$ remain authentic single bonds in both cases. Intermolecular interactions are observed in the solid state which result in the formation of pseudo-dimers (Fig. 2). The N–H and O parts of the uncoordinated side of $\mathbf{Q^2}_{\text{-H}}$ of one of the molecules forms intermolecular hydrogen bonding with the O and N–H part, respectively of a second molecule. The N–H distance is 0.730 Å and the H–O distance is 2.312 Å. The N–H–O angle is 158.3°. Additionally, a C–H–π interaction is observed between the C–H part of the coordinated phenyl ring of the $\mathbf{az}_{\text{-H}}$ ligand of one molecule and the central ring of the $\mathbf{Q^2}_{\text{-H}}$ ligand of another molecule. This C–H–π interaction holds together two of the pseudo-dimers formed through the aforementioned N–H–O interactions (Fig. 2) thus forming an infinite layer. The C–H–π distance is 3.205 Å and the angle between the C–H group and the centroid of the $\mathbf{Q^2}_{\text{-H}}$ ligand is 110.9°

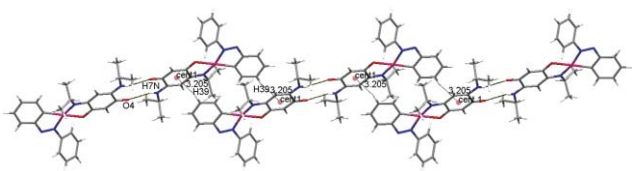

Fig. 2 Packing of the molecules of **2** in crystal showing hydrogen bonding and C–H–π interaction.

Cyclic voltammetry

Cyclic voltammetric measurements were carried out on the complexes in order to investigate their redox properties. The complexes **1** and **2** show irreversible oxidation processes at 0.58 and 0.80 V, respectively in CH_2Cl_2/0.1 M Bu_4NPF_6 *vs.* Fc^0/Fc^+. The reversibility of the processes did not improve upon lowering the temperature or varying the scan rate. Such processes with similar behavior were also observed in the case of the free ligands $\mathbf{Q^1}$ and $\mathbf{Q^2}$ (Table 3).[34] In view of these similarities and the fact that normally Pd(II) centres are usually resistant to reversible one-electron oxidation at reasonable potentials, we tentatively assign the oxidation process to the oxidation of the quinonoid ligands in the complexes. Its irreversibility has most likely to do with the N–H proton on the uncoordinated side of $\mathbf{Q^1}_{\text{-H}}$ and $\mathbf{Q^2}_{\text{-H}}$

Table 3 Electrochemical data[a]

Compound	E_{pa}(ox)[b]	$E_{1/2}$(red1)	$E_{1/2}$(red2)
$\mathbf{Q^1}$[c]	0.91	−1.64[d]	−2.24[d]
$\mathbf{Q^2}$[c]	0.89	−1.62[d]	−2.19[d]
1	0.58	−1.44	−1.75
2	0.80	−1.56	−1.85

[a] Electrochemical potentials from cyclic voltammetry in CH_2Cl_2/0.1 M Bu_4NPF_6 at 295 K. The Fc^0/Fc^+ couple was used as an internal standard. [b] Anodic peak potential for irreversible oxidation. [c] From ref. 31 [d] Cathodic peak potential for irreversible reduction.

ligands in the complexes **1** and **2**. In contrast to the oxidation process, the complexes **1** and **2** showed a fully reversible one-electron first reduction process at −1.44 and −1.56 V, respectively as well as a quasi-reversible second reduction process at −1.75 and −1.85 V, respectively (Fig. 3 and S1† and Table 3). It should be noted here that the reduction processes for the free ligands were not reversible.[34] Azo-based ligands are known to undergo two reversible one-electron reduction processes particularly in their metal-complexed form, as extensively studied with ligands such as phenylazopyridine (pap) or 2,2′-azobispyridine (abpy).[11,13] The first reduction potential of metal-bound azo ligands is generally at a lower negative potential and the difference between the two azo-based reduction processes is usually about 1 V.[11] Our own studies on the ligands $\mathbf{Q^1}$ and $\mathbf{Q^2}$ and their metal complexes have shown that such ligands are usually reduced at rather high negative potentials owing to the +I effects of the alkyl substituents and the difference between the two **Q** based reduction processes is usually around 600 mV (Table 3).[34,35] The difference between the two reduction processes for **1** and **2** are 310 mV and 290 mV, respectively. In view of this small difference and the trends in the reduction potentials of **az** and **Q** ligands mentioned above, we assign the first reduction process to the $\mathbf{az}_{\text{-H}}$ ligand resulting in the formation of species of the type $[(\mathbf{az}_{\text{-H}})^{\bullet-}\text{Pd}(\mathbf{Q}_{\text{-H}})]^{\bullet-}$ and the second reduction process to the $\mathbf{Q^1}_{\text{-H}}$ or $\mathbf{Q^2}_{\text{-H}}$ ligands

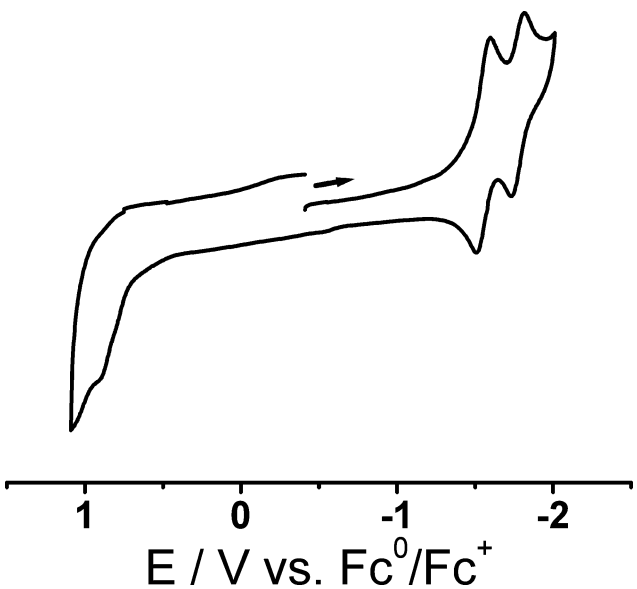

Fig. 3 Cyclic voltammogram of **2** in CH_2Cl_2/0.1 M Bu_4NPF_6 at 295 K. Scan rate 100 mV s^{-1}. The Fc^0/Fc^+ couple was used as an internal standard.

Table 4 UV-vis-NIR spectroelectrochemical data[a]

	λ_{max}/nm (ε/M^{-1}cm^{-1})
1	555(1200), 480sh, 407(19100), 360(20900)
1$^{\bullet-}$	1435(1700), 630sh, 553(3100), 397(20200), 362(18800)
1^{2-}	898(4600), 600sh, 487(5100), 382(15900), 337(13200)
2	560(820), 485sh, 407(17500), 359(20500)
2$^{\bullet-}$	1415(1650), 650sh, 557(3500), 397(19700), 360sh
2^{2-}	908(3400), 605sh, 490(4800), 386(12500), 329(14700)

[a] From OTTLE spectroelectrochemistry in CH_2Cl_2/0.1 M Bu_4NPF_6.

leading to the formation of [(**az**$_{\text{-H}}$)$^{\bullet-}$Pd(**Q**$_{\text{-H}}$)$^{\bullet-}$]$^{2-}$. In order to further verify this interpretation, we carried out UV-vis-NIR and EPR spectroelectrochemical measurements on these systems. The oxidation as well as the reduction potentials of the two complexes is rather similar as would be expected for similar electronic effects of the *n*-butyl and isopropyl substituents.

UV-vis-NIR and EPR spectroelectrochemistry

The complexes **1** and **2** show bands in the visible as well as ultraviolet regions in their native state in CH_2Cl_2/0.1 M Bu_4NPF_6 (Fig. 4 and S2† and Table 4). The lowest energy band at 555 nm for **1** and 560 nm for **2** is tentatively assigned to a mixture of ligand to ligand charge transfer (LLCT, **Q**$_{\text{-H}}$ → **az**$_{\text{-H}}$) and intra ligand charge transfer (ILCT, **Q**$_{\text{-H}}$ based). Confidence for the LLCT assignment comes from the ease of oxidation of the ligands **Q**$_{\text{-H}}$. The free ligands **Q**^{1} and **Q**^{2} also show absorptions in a similar region.[34] The bands at 480 nm for **1** and 485 nm for **2** are assigned to a metal to ligand charge transfer (MLCT, Pd → **az**$_{\text{-H}}$) and those at 407 for **1** and **2** are assigned to a second MLCT (Pd → **Q**$_{\text{-H}}$) transition. Further higher energy bands are assigned to intra ligand charge transfer (ILCT) transitions based on the **az**$_{\text{-H}}$ or **Q**$_{\text{-H}}$ ligands. Changes in the absorption patterns of **1** and **2** during the reduction processes were followed by using an optically transparent thin layer electrochemical (OTTLE) cell. On one electron reduction to **1**$^{\bullet-}$ or **2**$^{\bullet-}$ the original ILCT and MLCT bands in the visible region show a bathochromic shift and gain slightly in intensity (Fig. 4 and S2† and Table 4). In addition, a new broad band appears in the NIR region at 1435 and 1415 nm for **1**$^{\bullet-}$ and **2**$^{\bullet-}$, respectively. On one-electron reduction the **az**$_{\text{-H}}$-based lowest unoccupied molecular orbital (LUMO) of the starting complex will become the singly occupied molecular orbital (SOMO). This new transition is then assigned to a LLCT transition from SOMO(**az**$_{\text{-H}}$) → LUMO(**Q**$_{\text{-H}}$) in the one-electron reduced complexes (Fig. 4 and Scheme 3). These new LLCT bands are rather broad, the full width at half height ($\Delta\nu_{1/2}$) being 4075 and 4230 cm^{-1} for **1**$^{\bullet-}$ and **2**$^{\bullet-}$, respectively. The broadness probably originates from the reorganization in the system that would have to take place as a result of this transition between two different ligands. On further one-electron reduction to **1**$^{2-}$ or **2**$^{2-}$, the NIR band at around 1400 nm disappears and a new band emerges at 898 or 908 nm for **1**$^{2-}$ or **2**$^{2-}$, respectively. These are tentatively assigned to new MLCT transitions from Pd → **az**$_{\text{-H}}$. Further MLCT and ILCT transitions are seen at higher energies.

The *in situ* generated one-electron reduced species **1**$^{\bullet-}$ and **2**$^{\bullet-}$ in CH_2Cl_2/0.1 M Bu_4NPF_6 were probed with EPR spectroscopy to locate the site of electron transfer. The isotropic spectra for **1**$^{\bullet-}$ and **2**$^{\bullet-}$ at 295 K are centred at *g* values of 1.998 and 1.999, respectively (Fig. 5 and S3†). The resolution of the spectra was not ideal and hence only limits for the hyperfine coupling constants can be found from simulations. The spectra could be simulated by considering two different ^{14}N (I = 1) couplings of around 4.5 G and 6 G. Additionally, ^{105}Pd (I = 5/2, nat. abundance = 22.2%) satellites

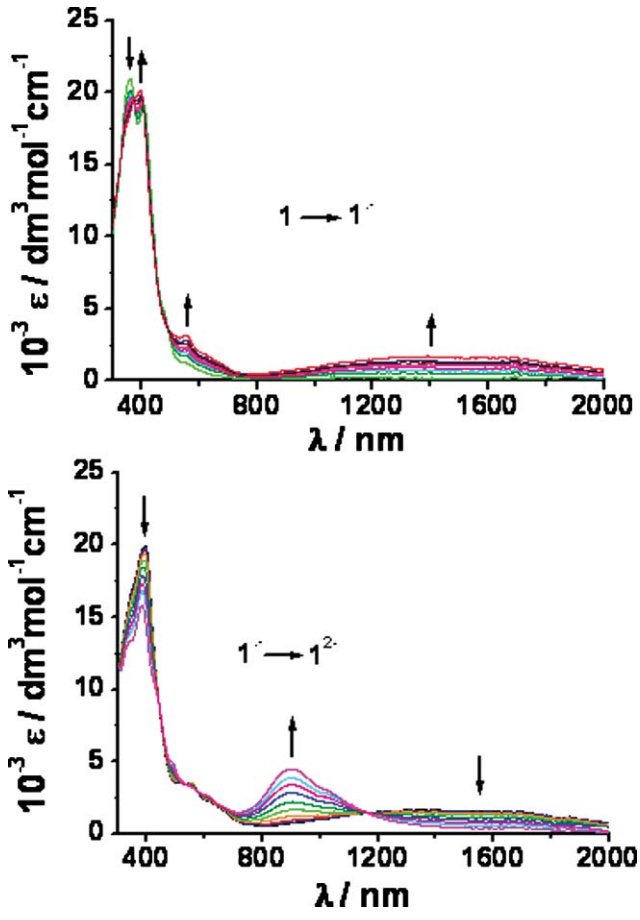

Fig. 4 Changes in the UV-vis-NIR spectrum of **1** during the reduction processes. From OTTLE spectroelectrochemistry in CH_2Cl_2/0.1 M Bu_4NPF_6.

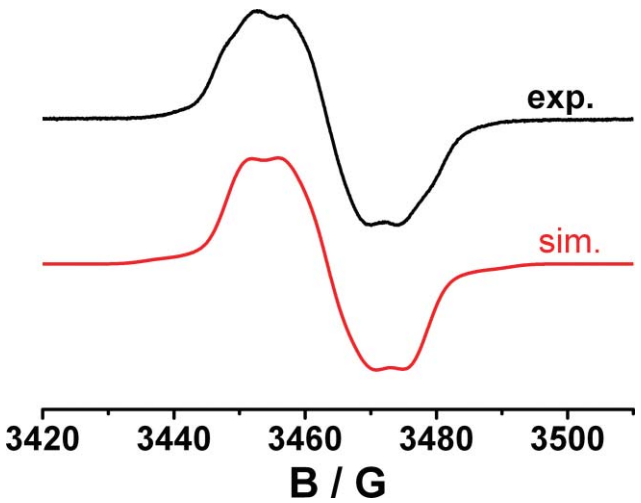

Fig. 5 EPR spectrum of *in situ* generated **1**$^{\bullet-}$ in CH_2Cl_2/0.1 M Bu_4NPF_6 at 295 K together with simulation.

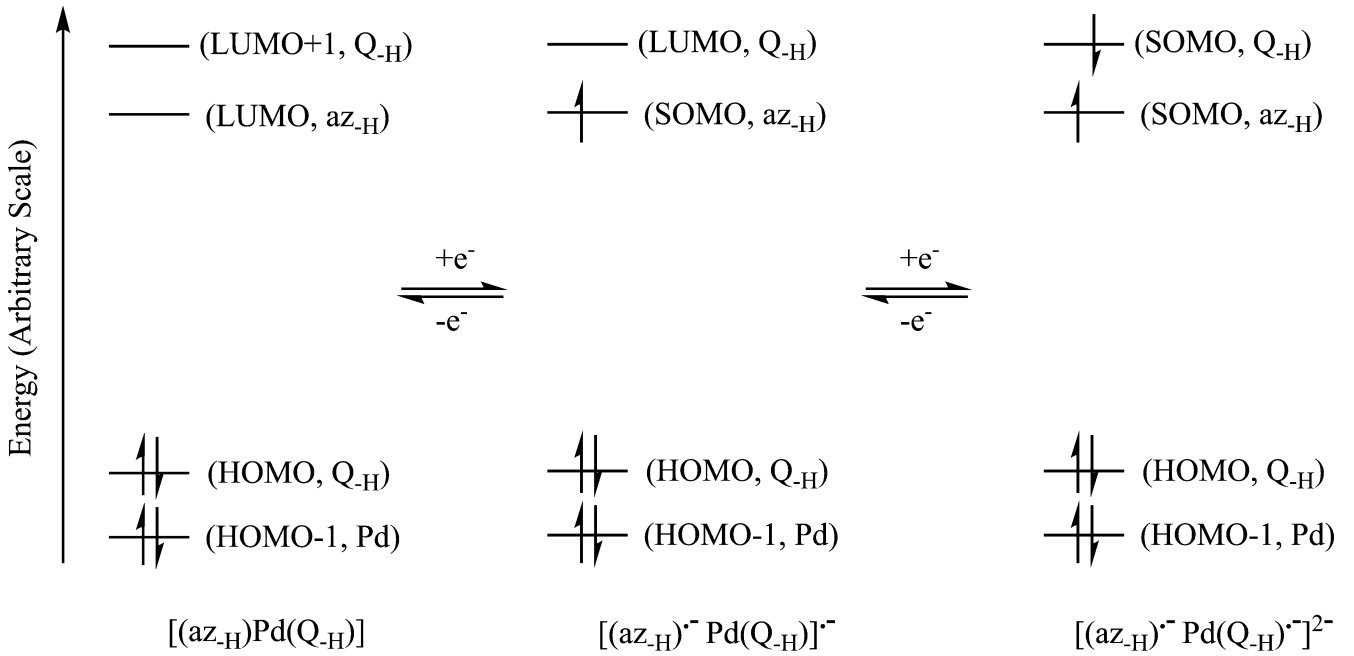

Scheme 3 Qualitative target orbitals for UV-vis-NIR transitions. Changes in orbital energies resulting from redox processes are not shown in this scheme.

of around 5 G can be seen at both extremities of the spectra. Thus these data point to a generation of a species of the form $[(\mathbf{az}_{\text{-H}})^{\bullet-}\text{Pd}(\mathbf{Q}_{\text{-H}})]^{\bullet-}$ on one-electron reduction. Further one-electron reduction to $\mathbf{1}^{2-}$ or $\mathbf{2}^{2-}$ leads to the spin-coupled diamagnetic singlet diradical of the form $[(\mathbf{az}_{\text{-H}})^{\bullet-}\text{Pd}(\mathbf{Q}_{\text{-H}})^{\bullet-}]^{2-}$ as seen by its EPR silence.

Conclusion

In summary, we have reported here on the synthesis of two new complexes **1** and **2**. Structural characterization of **2** showed features typical for metal bound $\mathbf{az}_{\text{-H}}$ ligands and mono-coordinated $\mathbf{Q}_{\text{-H}}$ ligands. A combination of electrochemical, UV-vis-NIR and EPR spectroelectrochemical studies have been used to show the stepwise reduction of the two different ligands leading first to a metal bound azo radical, $[(\mathbf{az}_{\text{-H}})^{\bullet-}\text{Pd}(\mathbf{Q}_{\text{-H}})]^{\bullet-}$ and then to a diamagnetic singlet diradical species, $[(\mathbf{az}_{\text{-H}})^{\bullet-}\text{Pd}(\mathbf{Q}_{\text{-H}})^{\bullet-}]^{2-}$. These complexes thus show double redox activity involving both coordinated ligands.

Experimental section

General considerations

The ligands $\mathbf{Q}^{\mathbf{1}}$ and $\mathbf{Q}^{\mathbf{2}}$ and the precursor complex $[\text{Pd}(\mu\text{-Cl})(\text{az}_{\text{-H}})]_2$ were prepared according to reported procedures.[4,34] All other reagents are commercially available and were used as received. All solvents were dried and distilled using common techniques unless otherwise mentioned. ^{1}H NMR spectra were recorded at 250.13 MHz on a Brucker AC250 instrument. EPR spectra in the X band were recorded with a Bruker System EMX. UV-Vis-NIR absorption spectra were recorded on a J&M TIDAS spectrophotometer. Cyclic voltammetry was carried out in 0.1 M Bu_4NPF_6 solution using a three-electrode configuration (glassy carbon working electrode, Pt counter electrode, Ag wire as pseudoreference) and PAR 273 potentiostat and function generator. The ferrocene/ferrocenium (Fc/Fc^+) couple served as internal reference. Elemental analysis was performed on a Perkin Elmer Analyser 240.

Synthesis

$[(\mathbf{az}_{\text{-H}})\text{Pd}(\mathbf{Q}^{\mathbf{1}}{}_{\text{-H}})]$, 1. A mixture of $\mathbf{Q}^{\mathbf{1}}$ (50 mg, 0.2 mmol) and KO*t*-Bu (24 mg, 0.2 mmol) in tetrahydrofuran (15 mL) was stirred for 8 h at room temperature. The solvent was removed *in vacuo*. The complex $[\text{Pd}(\mu\text{-Cl})(\text{az}_{\text{-H}})]_2$ (72 mg, 0.2 mmol) and dichloromethane (15 mL) were added to the orange precipitate. The reaction mixture was stirred for 3 h at room temperature. The colour of the solution changed to deep brown. The solvent was removed *in vacuo* and the product was extracted with *n*-hexane (20 mL) and filtered. The removal of the solvent of the filtrate *in vacuo* afforded the product as a brown solid. Yield: 56 mg (38%). ^{1}H NMR (250 MHz, CD_3CN): $\delta = 0.95$ (m, 6H, *n*-butyl), 1.38 (m, 4H, *n*-butyl), 1.65 (m, 4H, *n*-butyl), 3.24 (q, 2H, $J = 7.3$ Hz, *n*-butyl), 3.77 (broad s, 2H, *n*-butyl), 5.18 (s, 1H, N–C═C–H ring proton, $\mathbf{Q}^{\mathbf{1}}{}_{\text{-H}}$), 5.43 (s, 1H, O–C═C–H ring proton, $\mathbf{Q}^{\mathbf{1}}{}_{\text{-H}}$), 6.72 (broad s, 1H, NH), 7.37 (m, 3H, azobenzene), 7.54 (m, 3H, azobenzene), 7.90 (m, 2H, azobenzene), 8.02 (m, 1H, azobenzene). Anal. Calc. for $C_{26}H_{30}N_4O_2Pd$: C, 58.16; H, 5.63; N, 10.43. Found: C, 58.47; H, 5.58; N, 10.48.

$[(\mathbf{az}_{\text{-H}})\text{Pd}(\mathbf{Q}^{\mathbf{2}}{}_{\text{-H}})]$, 2. A mixture of $\mathbf{Q}^{\mathbf{2}}$ (46 mg, 0.2 mmol) and KO*t*-Bu (24 mg, 0.2 mmol) in tetrahydrofuran (15 mL) was stirred for 8 h at room temperature. The solvent was removed *in vacuo*. The complex $[\text{Pd}(\mu\text{-Cl})(\text{az}_{\text{-H}})]_2$ (72 mg, 0.2 mmol) and dichloromethane (15 mL) were added to the yellow precipitate. The reaction mixture was stirred for 3 h at room temperature. The colour of the solution changed to deep brown. The solution was filtered and *n*-hexane (10 mL) was added to precipitate the product. The precipitate was filtered, washed with *n*-hexane and dried *in vacuo*. Yield: 56 mg (55%). ^{1}H NMR (250 MHz, CD_3CN): δ = 1.24 (s, 3H, iso-propyl), 1.27 (s, 3H, iso-propyl), 1.51 (s, 3H, iso-propyl), 1.54

(s, 3H, iso-propyl), 3.72 (q, 1H, ^3J = 6.9 Hz, iso-propyl), 4.37 (q, 1H, ^3J = 6.9 Hz, iso-propyl), 5.21 (s, 1H, N–C═C–H ring proton, $\mathbf{Q^2_{-H}}$), 5.47 (s, 1H, O–C═C–H ring proton, $\mathbf{Q^2_{-H}}$), 6.49 (s, 1H, NH), 7.36 (m, 2H, azobenzene), 7.54 (m, 4H, azobenzene), 7.91 (m, 2H, azobenzene), 8.02 (m, 1H, azobenzene). Anal. Calc. for $C_{24}H_{26}N_4O_2Pd$: C, 56.64; H, 5.15; N, 11.01. Found: C, 56.58; H, 5.40; N, 11.20.

X-ray Ccrystallography

Single crystals of **2** were grown by slow evaporation of a 1 : 4 dichloromethane–*n*-hexane solution at ambient temperatures. The asymmetric unit consists of two molecules. X-ray diffraction data were collected using an OXFORD XCALIBUR-S CCD single crystal X-ray diffractometer. The structures were solved and refined by full-matrix least-squares techniques on F2 using the SHELX-97 program.[41] The absorption correction was done by the multi-scan technique. All data were corrected for Lorentz and polarization effects, and the non-hydrogen atoms were refined anisotropically. One of the isopropyl groups attached to the nitrogen atom is disordered.

Acknowledgements

BS is indebted to the Baden–Württemberg Stiftung for financial support of this work through the Elite Program for Postdocs. Denis Bubrin is kindly acknowledged for help with crystal structure solving.

References

1 H. Kirsch and P. Holzmeier, *Adv. Organomet. Chem.*, 1992, **34**, 67.
2 T. Yukuta, I. Mori, M. Kurihara, J. Mizutani, N. Tamai, T. Kawai, M. Irie and H. Nishihara, *Inorg. Chem.*, 2002, **41**, 7143.
3 S. Kume and H. Nishihara, *Dalton Trans.*, 2008, 3260.
4 A. C. Cope and R. W. Siekman, *J. Am. Chem. Soc.*, 1965, **87**, 3272.
5 D. Babic, M. Curic, K. Molcanov, G. Ilc and J. Plavec, *Inorg. Chem.*, 2008, **47**, 10446.
6 B. Sarkar, S. Patra, J. Fiedler, R. B. Sunoj, D. Janardanan, G. K. Lahiri and W. Kaim, *J. Am. Chem. Soc.*, 2008, **130**, 3532.
7 B. Sarkar, S. Patra, J. Fiedler, R. B. Sunoj, D. Janardanan, S. M. Mobin, M. Niemeyer, G. K. Lahiri and W. Kaim, *Angew. Chem., Int. Ed.*, 2005, **44**, 5655.
8 B. K. Santra, G. A. Thakur, P. Ghosh, A. Pramanik and G. K. Lahiri, *Inorg. Chem.*, 1996, **35**, 3050.
9 G. K. Lahiri, S. Bhattacharya, S. Goswami and A. Chakravorty, *J. Chem. Soc., Dalton Trans.*, 1990, 561.
10 S. Patra, B. Sarkar, S. Maji, J. Fiedler, F. A. Urbanos, R. J.-. Aparicio, W. Kaim and G. K. Lahiri, *Chem.–Eur. J.*, 2006, **12**, 489.
11 B. Sarkar, R. Huebner, R. Pattacini and I. Hartenbach, *Dalton Trans.*, 2009, 4653.
12 A. Dogan, B. Sarkar, A. Klein, F. Lissner, T. Schleid, J. Fiedler, S. Zalis, V. K. Jain and W. Kaim, *Inorg. Chem.*, 2004, **43**, 5973.
13 W. Kaim, *Coord. Chem. Rev.*, 2001, **219–221**, 463.
14 M. D. Ward and J. A. McCleverty, *J. Chem. Soc., Dalton Trans.*, 2002, 275.
15 A. I. Poddel'sky, V. K. Cherkasov and G. A. Abakumov, *Coord. Chem. Rev.*, 2009, **253**, 291.
16 C. G. Pierpont, *Coord. Chem Rev.*, 2001, **216–217**, 95.
17 P. Zanello, *Coord. Chem. Rev.*, 2006, **250**, 2000.
18 K. Ray, T. Petrenko, K. Wieghardt and F. Neese, *Dalton Trans.*, 2007, 1552.
19 M. Nomura, T. Cauchy and M. Fourmigué, *Coord. Chem. Rev.*, 2010, **254**, 1406.
20 B. Garreau de Bonneval, K. I. M.-C. Ching, F. Alary, T.-T. Bui and L. Valade, *Coord. Chem. Rev.*, 2010, **254**, 1457.
21 J. S. Miller and K. S. Min, *Angew. Chem., Int. Ed.*, 2009, **48**, 262.
22 S. Kitagawa and S. Kawata, *Coord. Chem. Rev.*, 2002, **224**, 11.
23 H. S. Das, F. Weisser, D. Schweinfurth, C.-Y. Su, L. Bogani, J. Fiedler and B. Sarkar, *Chem.–Eur. J.*, 2010, **16**, 2977.
24 O. Siri, P. Braunstein, M.-M. Rohmer, M. Benard and R. Welter, *J. Am. Chem. Soc.*, 2003, **125**, 13793.
25 O. Siri, J.-P. Taquet, J.-P. Collin, M.-M. Rohmer, M. Bénard and P. Braunstein, *Chem.–Eur. J.*, 2005, **11**, 7247.
26 O. Siri and P. Braunstein, *Chem. Commun.*, 2002, 208.
27 P. Braunstein, O. Siri, J.-P. Taquet, M.-M. Rohmer, M. Benard and R. Walter, *J. Am. Chem. Soc.*, 2003, **125**, 12246.
28 Q. Z. Yang, O. Siri and P. Braunstein, *Chem. Commun.*, 2005, 2660.
29 Q. Z. Yang, O. Siri and P. Braunstein, *Chem.–Eur. J.*, 2005, **11**, 7237.
30 J.-P. Taquet, O. Siri, P. Braunstein and R. Welter, *Inorg. Chem.*, 2004, **43**, 6944.
31 Q. Z. Yang, A. Kermagoret, M. Agostinho, O. Siri and P. Braunstein, *Organometallics*, 2006, **25**, 5518.
32 F. A. Cotton, J.-Y. Jin, Z. Li, C. A. Murillo and J. H. Reibenspies, *Chem. Commun.*, 2008, 211.
33 H. S. Das, A. K. Das, R. Pattacini, R. Huebner, B. Sarkar and P. Braunstein, *Chem. Commun.*, 2009, 4387.
34 P. Braunstein, D. Bubrin and B. Sarkar, *Inorg. Chem.*, 2009, **48**, 2534.
35 A. Paretzki, R. Pattacini, R. Huebner, P. Braunstein and B. Sarkar, *Chem. Commun.*, 2010, **46**, 1497.
36 H.-Y. Cheng, G.-H. Lee and S.-M. Peng, *Inorg. Chim. Acta*, 1992, **191**, 25.
37 S. Scheuermann, T. Kretz, H. Vitze, J. W. Bats, M. Bolte, H.-W. Lerner and M. Wagner, *Chem.–Eur. J.*, 2008, **14**, 2590.
38 W.-G. Jia, Y.-F. Han, Y.-J. Lin, L.-H. Weng and G.-X. Jin, *Organometallics*, 2009, **28**, 3459.
39 J. Mattsson, P. Govindaswamy, A. K. Renfrew, P. J. Dyson, P. Stepnicka, G. S. Fink and B. Therrien, *Organometallics*, 2009, **28**, 4350.
40 S. Kar, B. Sarkar, S. Ghumaan, D. Janardanan, J. van Slageren, J. Fiedler, V. G. Puranik, R. B. Sunoj, W. Kaim and G. K. Lahiri, *Chem.–Eur. J.*, 2005, **11**, 4901.
41 G. M. Sheldrick, '*SHELXS-97, Program for Solution of Crystal Structures*', University of Göttingen, Germany, 1997.

